

Synthesis, Characterization, and Small Hydrocarbon Encapsulation of Dicavitand-Porphyrins

Jun Nakazawa,*[1] Jun Hagiwara,[2] Yuichi Shimazaki,[3] Fumito Tani,[2] and Yoshinori Naruta*[2]

[1]Department of Material and Life Chemistry, Faculty of Engineering, Kanagawa University, 3-27-1 Rokkakubashi, Kanagawa-ku, Yokohama, Kanagawa 221-8686

[2]Institute for Materials Chemistry and Engineering, Kyushu University, 6-10-1 Hakozaki, Higashi-ku, Fukuoka 812-8581

[3]Department of Science, College of Science, Ibaraki University, 2-1-1 Bunkyo, Mito, Ibaraki 310-8512

Received April 5, 2012; E-mail: jnaka@kanagawa-u.ac.jp

New host molecules "Dicavitand-Porphyrins" [H_2**C$_2$P**(syn,syn) (**3**), H_2**C$_2$P**(syn,anti) (**4**)] with small cavities on one or both sides of the porphyrin plane were synthesized from 5,10-bis(2,6-dihydroxyphenyl)-15,20-diphenylporphyrin and bis(chloromethyl)cavitand in 15 and 34% yield, respectively. Similarity of guest size selectivity of the host **4** in comparison with the reported "Cavitand-porphyrin" [H_2**CP**(syn) (**1**)] suggests that these hosts have the same cavity size. The 1:1 and 1:2 association constants (K_{11} and K_{12}) of the guest encapsulations into **3** were also obtained by ^{1}H NMR titration and nonlinear least square fittings. The guest size dependences of K_{11} and K_{12} values of **3** show that the initial cavity prefers larger guests such as ethane, while the second one does not. The induced-fit type very small structural changes (estimated within 1 Å) upon first guest encapsulation of the host **3** affects the guest encapsulation of the other cavity through the covalent linkages.

The encapsulation of small molecules is an important research area of molecular recognition chemistry for applications such as gas storage, sensors, and chemoselective reactions within the host cavities, as well as the basic study of weak intermolecular interactions.[1–7] In terms of small molecules, hydrocarbons are one of the most difficult guests to target for recognition, as they lack functionalities that form strong interactions with host molecules. To encapsulate small hydrocarbon molecules reversibly, it is necessary to prepare cavities that have suitable pore sizes for guests and flexible gate system.[8–26] The size relation between host cavity and guests has been studied by many researchers especially by Rebek and co-workers.[27] To improve the versatility and applicability of encapsulation systems, an additional substituent group or a triggering event in the host system is needed to be built in.[3,28–38] Multiple guest encapsulations in one host molecule is one of the methods, and has many potential benefits: (1) Increased guest capacity for molecular storage applications.[39–41] For example, Atwood and co-workers reported that multiple small molecule storage in resorcin[4]arene crystals.[42,43] (2) Selective reactivity between encapsulated guests in host cavities termed molecular reaction flasks.[4,44,45] (3) Guest selectivity control upon addition of external stimuli for "smart" sensor applications.[46] Rebek and co-workers reported a coencapsulation method that changed the selectivity for the second guest within the large cavity of the cylindrical molecular capsule by decreasing the cavity volume though addition of the first guest.[47–53] In addition, the guest selectivity change via the cavity size control using addition of spacers has been reported.[54–57]

In our previous studies, we had synthesized capsule-like hosts "Cavitand-Porphyrin" H_2**CP**(syn) (**1**, structure is shown in Figure 1) which has a small cavity at one side of the porphyrin plane and had investigated encapsulation of small molecules into this capsule cavitiy.[58–61] The cavity shows high affinity for small hydrocarbons such as methane and ethane. In addition, we also reported induced-fit-type structural change of the capsule upon the guest encapsulation. We considered that the very small structural change (estimated within 1 Å) of the host can be used as a stimulus to multiguests encapsulation. Similar strategy is known in biological systems such as the allosteric effect of oxygen binding of hemoglobin by protein structural change.[62,63]

In this article, we aimed to change affinity for a second guest by a host structural change upon first guest encapsulation. We synthesized new host molecules H_2**C$_2$P**s having two cavitands and a porphyrin similar to reported H_2**CP**s **1** and **2**. This H_2**C$_2$P**s are considered to have three structural isomers (syn,syn; **3**), (syn,anti; **4**), and (anti,anti; **5**) with respect to orientation of the two cavitand groups, as shown in Figure 1. The (syn,syn) isomer **3**, of H_2**C$_2$P**s has a cavity on either sides of the porphyrin plane, and both cavitands were connected by two 2,6-dihydroxyphenyl groups at 5,15-meso-position of the porphyrin. We expected that a structural change of the cavities through these linkers upon encapsulation of the first guest would alter the selectivity for second guest encapsulation.

Results and Discussion

Synthesis of H_2C$_2$Ps. As the precursor of the cavitand moiety of H_2**C$_2$P**, bis(chloromethyl)cavitand **6** was synthesized based on a previous report.[59] To prepare the porphyrin part, a mixture of *meso*-bis(2,6-dimethoxyphenyl)diphenylporphyrin (**7**) was synthesized from mixed condensation of

Published on the web August 3, 2012; doi:10.1246/bcsj.20120107

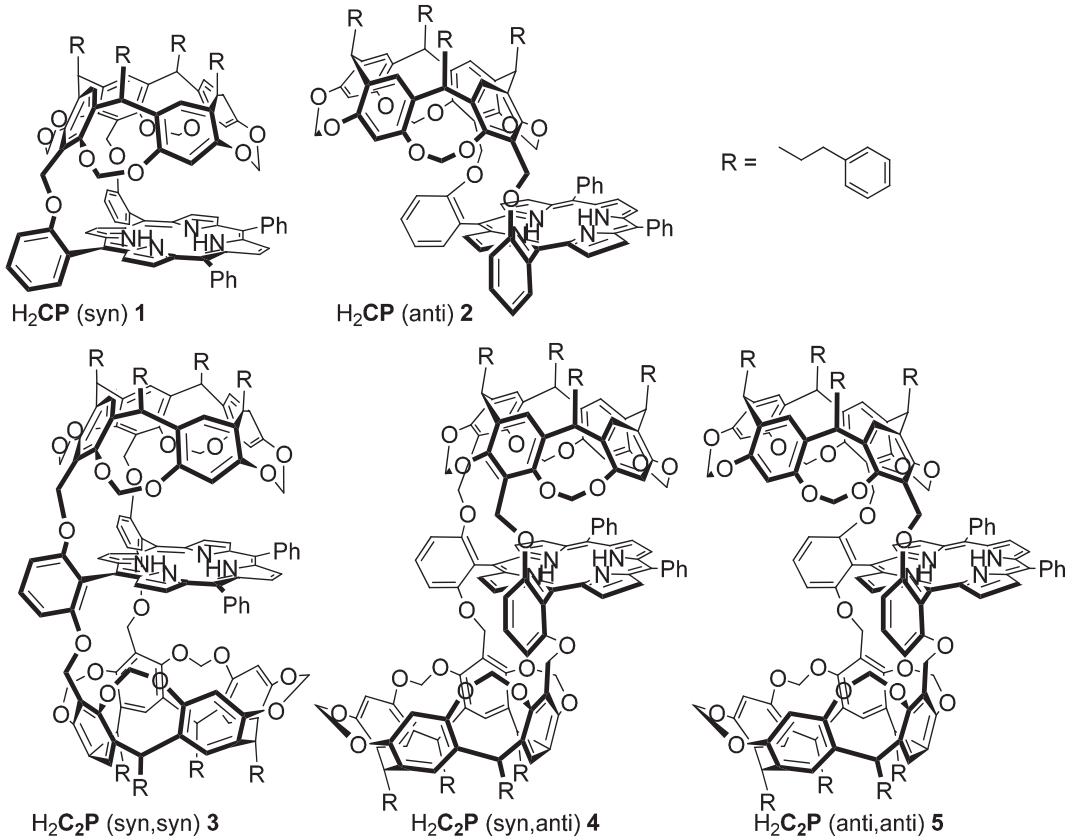

Figure 1. Structures of H_2**CP**s **1** and **2** and H_2**C$_2$P**s **3**, **4**, and **5**.

2,6-dimethoxybenzaldehyde, benzaldehyde, and pyrrole with Montmorillonite K10 as a heterogeneous acid catalyst, and subsequent in situ oxidation by 2,3-dichloro-5,6-dicyano-1,4-benzoquinone (DDQ) in 19% yield.[64] Since the separation of the 5,10- and 5,15-disubstituted porphyrin isomers is difficult by silica gel column chromatography, the mixture was directly used in the next step. The methyl groups in compound **7** were removed by pyridine hydrochloride at 210 °C. 5,10-Bis(2,6-dimethoxyphenyl)-15,20-diphenylporphyrin (**8**) was obtained in 46% yield by silica gel column chromatography to remove 5,15-isomer and their decomposed by-products.

Synthesis of H_2**C$_2$P**s were carried out by similar procedure of reported H_2**CP**s, **1** and **2** (Figure 2).[59] TLC analysis (silica gel, benzene) of crude product showed two new low-polarity reddish-purple spots (more polar spot; **4**, the other spot; **3**). These products were separated by silica gel column chromatography. Since HR-MS spectra and elemental analyses of compound **3** and **4** show good correlations with the dicavitand-porphyrin formula, we determined that **3** and **4** were structural isomers of H_2**C$_2$P**s. To distinguish structure of isomers **3** and **4**, we obtained these 1D-^{1}H and ^{1}H–^{1}H COSY NMR spectra. The ^{1}H NMR spectra of **3** shows a more symmetric pattern than that of **4** and similar to that of H_2**CP**(syn) (**1**). On the other hand, the ^{1}H NMR signal pattern of **4** correlates to a 1:1 mixture of **1** and **2**. Thus compound **3** was characterized as H_2**C$_2$P**(syn,syn) that has two cavitands covering the porphyrin, and compound **4** was characterized as H_2**C$_2$P**(syn,anti) that has only one cavitand covering the porphyrin, respectively. The polarity of H_2**C$_2$P**s in TLC analysis (**4** is polar than **3**) also supports this

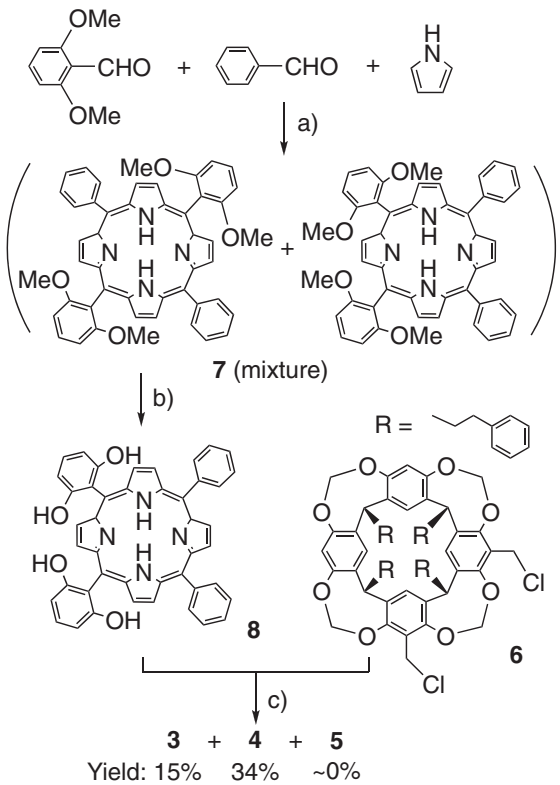

Figure 2. Synthesis of H_2**C$_2$P**s. a) (1) Montmorillonite K10, CH_2Cl_2, RT, overnight. (2) DDQ, CH_2Cl_2, RT, 1 h, 19%. b) Py·HCl, 210 °C, 2 h, 47%. c) K_2CO_3, THF/NMP, 120 °C, 4 d.

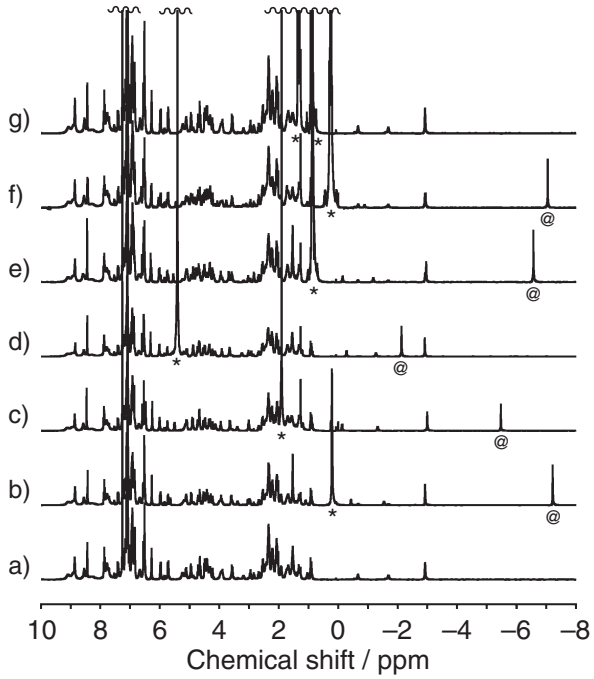

Figure 3. ^{1}H NMR spectra of small hydrocarbons encapsulation into **4** in $CDCl_3$ at 25 °C. a) Free **4**, b) methane, c) acetylene, d) ethylene, e) ethane, f) cyclopropane, g) *n*-propane. @: encapsulated guest signals, *: free guest signals.

characterization according to the H_2**CP** case. The syn isomer **1** of H_2**CP** shows less polarity than the anti isomer **2** in TLC analysis (silica gel, benzene), because of the –O–CH_2–O– groups at the rim of the cavitand in syn form are covered by the porphyrin plane to prevent interaction with the silica gel surface. It is worth mentioning that the isomer **5** is not formed under current reaction condition. The yields of isomers [**3** (15%), **4** (34%), and **5** (0%)] may correlate to degree of structural strain around the hinges of the intermediates in the transition state of the irreversible ring closure process, and the "strainless" (syn,anti) transition intermediate may convert to the strainless product **4**. In addition, the yields also show that structural orientation of one cavitand affects to the cavitand on the other side through restricted rotation of the two *meso*-phenyl linkers of the porphyrin connecting the two cavitands. It is easy to imagine that the structural effect causes difference in guest encapsulation affinity between the two cavities of **3**.

Encapsulation of Small Hydrocarbons into the Host 4. The H_2**C$_2$P**(syn,anti) (**4**) has a cavity suitable for small guest encapsulation at one side (syn side) of the porphyrin. The encapsulations of small hydrocarbon guests into the cavity of **4** were observed by ^{1}H NMR in $CDCl_3$ at 25 °C, as shown in Figure 3. Upon bubbling of methane gas into the 5 mM solution of **4**, a new signal appeared at −7.22 ppm in addition to a free methane signal at 0.15 ppm (Figures 3a to 3b). We characterized the new signal of the methane/**4** system as the encapsulated methane in the syn side cavity. This signal correlates with the reported methane/**1** system which shows an encapsulated methane signal at −7.15 ppm under the same condition (Table 1).[59] The signal shift magnitude ($\Delta\delta = -7.37$ ppm) between free and encapsulated methane in **4** is slightly

Table 1. ^{1}H NMR Chemical Shifts (ppm) of Encapsulated Hydrocarbons into **1**, **3**, and **4** in $CDCl_3$ at 25 °C

Guest	Free	**1**[a)]	**3** (1:1)	**3** (1:2)	**4**
Methane	0.15	−7.19	−7.37	−7.36	−7.22
Acetylene	1.91	−5.37	−5.80	−5.72	−5.47
Ethylene	5.39	−2.07	−2.31	−2.24	−2.13
Ethane	0.85	−6.49	−6.72	−6.65	−6.57
Cyclopropane	0.23	−6.95	−7.21	−7.11	−7.05
n-Propane	1.31, 0.88	—[b)]	—[b)]	—[b)]	—[b)]

a) From Ref. 59. b) Not encapsulated.

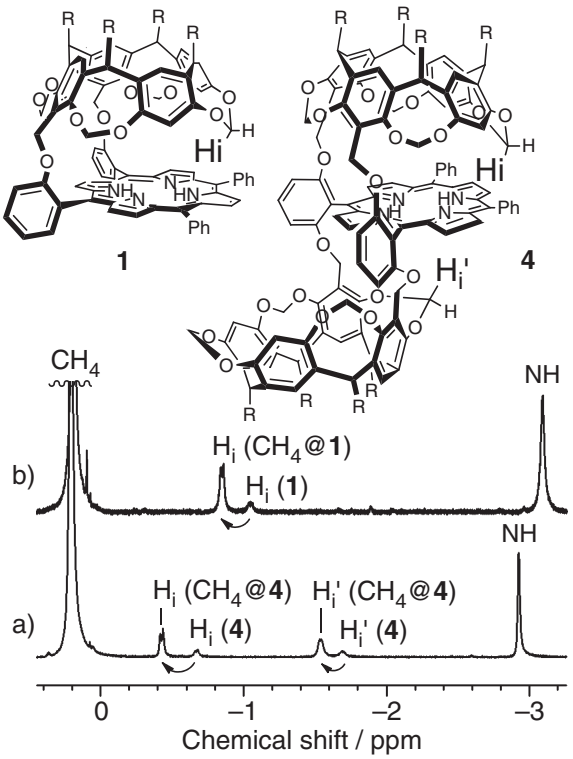

Figure 4. The H_i signal shifts of a) **4** and b) **1** upon methane encapsulation in ^{1}H NMR in $CDCl_3$ at 25 °C.

larger than that of methane/**1** system ($\Delta\delta = -7.34$ ppm). This shift seen in **4** is caused by additional shielding from the cavitand on the other side of the porphyrin plane. In our earlier work, we reported that the H_i signal in host **1** shifts downfield upon encapsulation of methane, due to structural change of the cavity. In the case of **4**, H_i signal also shifts downfield. In addition, we can see that H_i' signal of **4** (the proton located on the anti side cavitand) shifts downfield (Figure 4). H_i' shows that a structural change in the syn side cavity upon encapsulation of methane affects the structure of the anti side cavitand through the two covalent linkers connecting the two cavitands.

New signals appeared at the extremely high field region upon addition of small hydrocarbons such as acetylene, ethylene, ethane, and cyclopropane by bubbling into the $CDCl_3$ solution of **4**. In contrast, addition of larger hydrocarbons than the above guests, such as propane does not show any new signals except for the free propane signals. Thus the cavity of **4** can encapsulate small hydrocarbons from methane up to cyclopropane, size selectively. Since the host **1** can also encap-

sulate small hydrocarbons up to cyclopropane, host **1** and **4** have almost the same size cavity.

To obtain further information on guest selectivity of host **4**, we carried out guest titrations and calculated 1:1 association constants K_{11} of **4** using eq 1. The K_{11} values of small hydrocarbon guests/**4** system and the plot for the methane/**4** system are shown in Table 2 and Figure S1, respectively. The isomer **4** has similar K_{11} values and trend for guest selectivity (that is high affinities for methane and acetylene) to isomer **1**, suggesting that **1** and **4** have similar size cavities. This cavity size similarity also shows that the additional cavitand at the anti side of the host **4** makes no steric distortion of the syn side cavity through two linkers that connect the syn and anti cavitands.

Encapsulation of Small Hydrocarbons into 3. Encapsulation of small hydrocarbon molecules into host **3** was monitored by ^{1}H NMR titrations. Change in ^{1}H NMR spectrum upon addition of methane into 2 mM $CDCl_3$ solution of **3** is shown in Figure 5. A new signal appears at −7.37 ppm that initially increases in intensity with addition of small amount of methane. Upon further addition of methane, this signal starts decreasing in intensity while another new signal that continues to increase appears on the shoulder of the first signal at −7.36 ppm. Since the host **3** has two small cavities at both sides of the porphyrin plane, we characterized the first new signal at −7.37 ppm and the second signal at −7.36 ppm as encapsulated methane protons of the 1:1 and 1:2 association modes, respectively (Table 1). Due to the structure of 1:2 association mode has mirror plane symmetry with respect to the porphyrin plane within the NMR time scale, the signals of two encapsulated methane molecules in cavitands on either side appeared at the same chemical shift −7.36 ppm. In addition, the 1:2 signal appearing downfield of the 1:1 signal may be caused by decreasing shielding of the cavitand and the porphyrin by enlarging both cavities upon the second guest encapsulation. Since methane is the smallest guest we used, the shift magnitude of encapsulated methane signals between 1:1 and 1:2 modes of the methane/**3** system is small compared to other guests.

Table 2. The 1:1 and 1:2 Association Constants (K_{11} and K_{12}, M^{-1}) of Hydrocarbons Encapsulation into **1**, **3**, and **4** in $CDCl_3$ at 25 °C Obtained by ^{1}H NMR Titrations

Guest	**1** (K_{11})[a)]	**3** (K_{11})	**3** (K_{12})	**4** (K_{11})
Methane	81 ± 18	257 ± 21	136 ± 12	108 ± 5
Acetylene	130 ± 20	707 ± 40	201 ± 12	141 ± 5
Ethylene	49 ± 5	281 ± 20	182 ± 14	55 ± 3
Ethane	9 ± 1	135 ± 9	16 ± 1	9 ± 1
Cyclopropane	10 ± 2	179 ± 5	11 ± 1	4 ± 1

a) From Ref. 59.

The encapsulation of other small hydrocarbons into **3** was also monitored by ^{1}H NMR titration. The cavities of **3** can encapsulate small hydrocarbon guests from methane to cyclopropane in similar fashion to hosts **1** and **4**, as determined by the appearance of a new ^{1}H NMR signal at extreme high field (Table 1). The spectral change upon addition of ethane into a $CDCl_3$ solution of **3** is shown in Figure 6 as an example, and spectral changes upon addition of acetylene, ethylene, cyclopropane, and propane are shown in Figures S2–S5 in the Supporting Information. Upon the addition of a small amount of ethane gas into a $CDCl_3$ solution of **3** (2 mM), a new signal appeared at −6.72 ppm in the ^{1}H NMR spectrum. By increasing concentration of ethane, the signal intensity changes, increasing at first and then decreasing. The decrease of the signal at −6.72 ppm corresponds with the appearance of a new signal at −6.65 ppm. We ascribe the pattern of ^{1}H NMR signals to the encapsulation of ethane in **3** in a 1:1 and 1:2 ratio. In methane/**3** system, the chemical shift difference between the encapsulated methane signals of 1:1 and 1:2 modes is very small ($\Delta\delta$ = 0.01 ppm), and a host signal at 6.3 ppm shows no change. In contrast, the shift difference of encapsulated ethane is large ($\Delta\delta$ = 0.07 ppm), and the host signal at 6.3 ppm also shifts

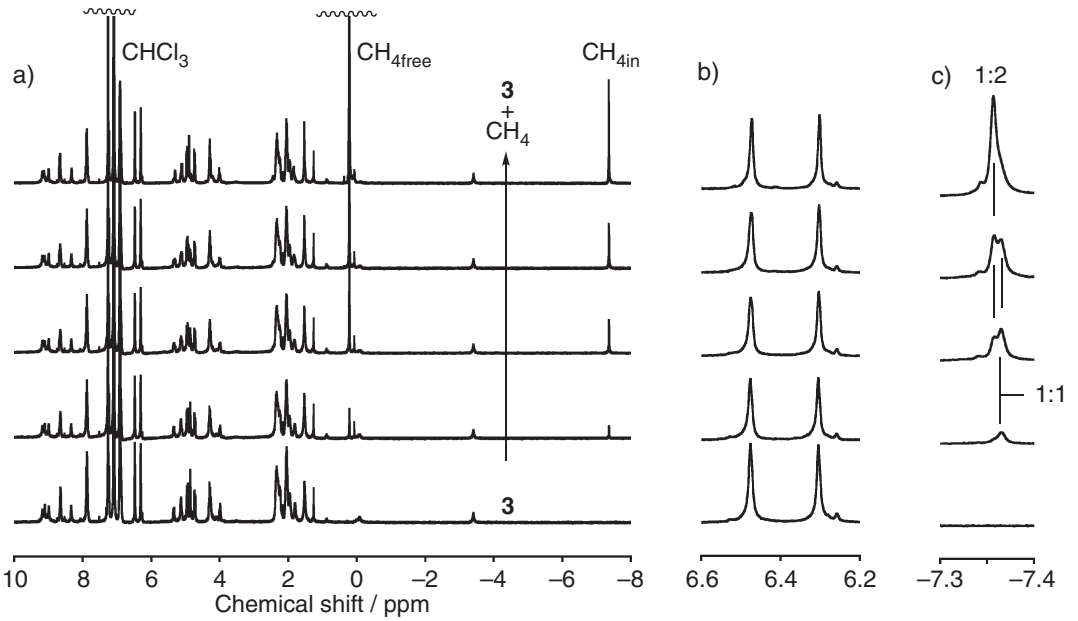

Figure 5. ^{1}H NMR spectral changes of **3** upon addition of methane in $CDCl_3$ at 25 °C. a) Full spectra, b) selected expanded view of host signals (6.2–6.6 ppm), and c) expanded view of the signals of encapsulated methane.

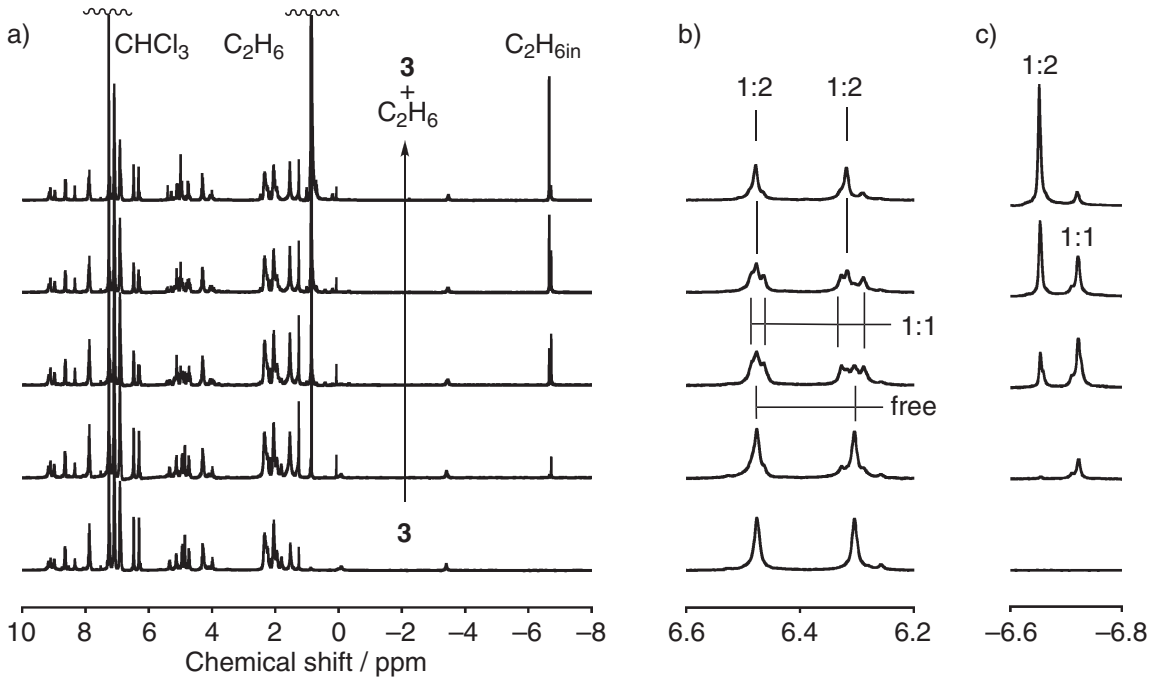

Figure 6. ^{1}H NMR spectral changes of **3** upon addition of ethane in $CDCl_3$ at 25 °C. a) Full spectra, b) selected expanded view of host signals (6.2–6.6 ppm), and c) expanded view of the signals of encapsulated ethane.

upon the ethane encapsulation. The significant spectral change caused by structural reorganization upon ethane encapsulation is a result of the larger size of this guest in comparison to methane. The chemical shift difference between 1:1 and 1:2 modes (Table 1) and host signal changes (Supporting Information Figures S2–S5) correlate with guest size, with acetylene being the exception. The acetylene/**3** system shows a different trend; a large chemical shift difference of the 1:1 and 1:2 encapsulated acetylene signals, and in addition, a significant chemical shift change of N–H proton signals of the host porphyrin. The specific difference may caused by the acidic character of acetylene C–H.[65]

The ^{1}H NMR spectral differences between the 1:1 and 1:2 association modes of guest/**3** systems can be attributed to a host structural change upon encapsulation of the first guest. We expected that this host structural change upon encapsulation of the first guest would influence the second association process. To check the guest association affinity of **3**, we carried out titrations of intensity change of the guest ^{1}H NMR signal at different guest concentrations. The 1:1 and 1:2 association constants for various guests with the host **3** were obtained by nonlinear least square fitting using eq 7 (Figure S6). Due to overlap of the 1:1 and 1:2 encapsulated methane signals, we used the sum concentration $[G]_{in}$ of the 1:1 and 1:2 encapsulated guests for the calculation. In the methane/**3** system, the titration was hampered before full encapsulation by the low solubility of methane in $CDCl_3$. Generally, these limitations decrease accuracy of K_{12} values. In addition, we could not titrate to the endpoint (full encapsulation) due to the low affinity of **3** for these guests in ethane/**3** and cyclopropane/**3** systems. The calculated values of K_{11} and K_{12} are shown in Table 2. In contrast to hosts **1** and **4** those have high affinities for smaller guests such as methane and acetylene, the initial guest encapsulation of host **3** shows higher affinities for bigger guests by the comparison of the K_{11} values. The guest affinity trend for **3** depends on guest hydrocarbon size and is relatively similar to that of a hydrogen bonding type **CA-PyP** host[60] which has a larger cavity than **1** (K_{11} for methane = 56, acetylene = 202, ethylene = 690, ethane = 527, and *n*-propane = 236 M^{-1}). The high affinity for larger guest supposes that the range of motion of the hinges connecting the porphyrin and the cavitands in host **3** are different to that of host **1**. Generally, initial and second binding events of a host having two "independent" sites follow statistics in a K_{12}/K_{11} ratio of 0.25.[66] The K_{12}/K_{11} ratios for encapsulations of smaller guests such as methane (0.53), acetylene (0.28) and ethylene (0.64) into the host **3** are larger than 0.25 indicating that the cavities of the host show positive cooperativity for these smaller guests. Upon increasing of guest size up to ethane ($K_{12}/K_{11} = 0.11$) and cyclopropane (0.06), the cooperativity between the cavities of the host **3** turns to the opposite negative direction. The van der Waals interaction between such larger initial guest and the porphyrin plane tilts the porphyrin toward the second free cavity side. This affinity change can be categorized to a kind of allosteric effect via induced-fit type host structural change with weak van der Waals interaction between a host and guests.

Conclusion

We have synthesized and studied encapsulation event of a series of host molecules (H_2**C$_2$P**s) with cavitands on either side of a porphyrin molecule, connected via the same *meso*-aromatic ring of the porphyrin. It was expected that the synthesis of H_2**C$_2$P**s would afford three structural isomers **3**(syn,syn), **4**(syn,anti), and **5**(anti,anti) due to a difference in cavitand direction. However, host **4** was generated in high yield than **3**, and compound **5** was not generated under our conditions.

We evaluated small hydrocarbon encapsulation into **4**, which has a cavity on the syn side of the porphyrin plane, with a reported similar host H_2**CP**(syn) (**1**). The host **4** exhibits the same trend of guest encapsulation properties as compared to **1**, demonstrating that the cavity structure on the syn side of **4** is very similar to **1**, because the anti-cavitand does not influence this binding process. In addition, we observed the NMR signal shifts of the H_i' proton of anti-cavitand caused by a structural change of guest encapsulation at syn side cavity through the two linkers.

Small hydrocarbon encapsulation into host **3**, which has cavities on either side of the porphyrin plane, was monitored by ^{1}H NMR titrations. We observed signals of free host, as well as the 1:1 and 1:2 association states separately by ^{1}H NMR spectra. The difference of encapsulated guest chemical shifts between 1:1 and 1:2 associations becomes larger with increasing guest size. This can be rationalized by the changing of magnetic shielding effect caused by induced-fit-type structural change of the host. This structural change accounts for the difference of guest encapsulation affinity of the free and 1:1 associated host **3**. The guest size dependences of K_{11} and K_{12} values of **3** show that the initial cavity prefers larger guests such as ethane, while the second one does not.

There are many reports that demonstrate an allosteric effect due to host structural changes using hydrogen or coordination bonds. In contrast, our system shows an allosteric effect via induced-fit-type host structural change with weak van der Waals interaction between a host and guests.

Experimental

Materials and Instruments. Commercially available reagents and solvents were used without further purification unless otherwise noted. Tetrahydrofuran (THF) was dried over KOH, and distilled from sodium diphenylketyl under N_2 atmosphere. *N*-Methylpyrrolidone (NMP) was dried over molecular sieves 4A for several days. $CDCl_3$ (99.8 atom % D, ACROS ORGANICS) was passed through an alumina column. Cavitand-Porphyrins (syn; **1**), (anti; **2**), and bis(chloromethyl)-cavitand **6** were synthesized according to literature.[59]

^{1}H NMR spectra were recorded on a JEOL JMX-GX400 (400 MHz) spectrometer. ^{1}H NMR chemical shifts (δ) are reported in parts per million (ppm) relative to TMS using the residual proton resonance of $CDCl_3$ ($\delta = 7.26$ ppm). High-resolution MS (HR-MS) spectra were recorded on a JEOL LMS-HX-110 spectrometer. FAB-MS spectra were measured with 3-nitrobenzyl alcohol as matrix.

Synthesis of *meso*-Bis(2,6-dimethoxyphenyl)-*meso*-Diphenylporphyrin (mixture of 5,10- and 5,15-isomers, 7). To a suspension of Montmorillonite K10 (10 g), 2,6-dimethoxybenzaldehyde (0.42 g, 2.5 mmol), and benzaldehyde (0.27 g, 2.5 mmol) in 100 mL of CH_2Cl_2, pyrrole (0.35 mL, 5.1 mmol) were added at RT under N_2 atmosphere. The reaction mixture was stirred for overnight and then DDQ (0.85 g, 3.7 mmol) were added. After stirring of the mixture for additional hour, Montmorillonite K10 was removed from the mixture by filtration and well washed with CH_2Cl_2. The filtrate was passed through an alumina column, and then the solvent was evaporated under reduced pressure. The residue was purified by silica gel column chromatography (benzene, third fraction band) to give **7** as a purple solid in 19% yield (0.16 g, 0.24 mmol). The product was dried in vacuo at room temperature for 3 h prior to the next reaction.

7: ^{1}H NMR ($CDCl_3$): δ 8.76 (m, 8H, pyrrole-β), 8.21 (d, $J = 7.6$ Hz, 4H, Ph-4), 7.73 (m, 8H, Ph-2,3,5,6 + $(OH)_2$Ph-4), 7.01 (d, $J = 8.4$ Hz, 4H, $(OH)_2$Ph-3,5), 3.52 + 3.51 (s + s, 12H, Me), −2.61 + −2.62 (s + s, 2H, NH). HR-MS ($C_{48}H_{38}N_4O_4$): m/z = calcd 734.2893, found 734.2888.

Synthesis of 5,10-Bis(2,6-dihydroxyphenyl)-15,20-diphenylporphyrin (8). The methoxy-substituted porphyrin **7** (120 mg, 160 μmol) was heated in excess pyridine hydrochloride for 2 h at 210 °C under N_2 atmosphere. After the mixture was cooled below 100 °C, the reaction mixture was treated with water. The residue was extracted with AcOEt, and the organic layer was washed with 0.1 M HCl, saturated solution of $NaHCO_3$ in water, and brine. The organic layer was dried with Na_2SO_4, and then the solvent was evaporated under reduced pressure. The residue was purified by silica gel column chromatography (CH_2Cl_2/AcOEt = 95/5–92/8, the second fraction band) to give **8** as a reddish purple solid in 46% yield (50 mg, 73.7 μmol). The product was dried in vacuo at 120 °C for 3 h prior to the next reaction.

8: ^{1}H NMR ($CDCl_3$): δ 8.99 (s, 2H, pyrrole-β), 8.94 (s, 4H, pyrrole-β), 8.88 (s, 2H, pyrrole-β), 8.21 (d, $J = 6.3$ Hz, 4H, Ph-4), 7.80 (m, 6H, Ph-2,3,5,6), 7.61 (t, $J = 8.3$ Hz, 2H, $(OH)_2$Ph-4), 6.97 (d, $J = 8.3$ Hz, 4H, $(OH)_2$Ph-3,5), 4.69 (br, 4H, OH), −2.71 (s, 2H, NH). HR-MS ($C_{44}H_{30}N_4O_4$): m/z = calcd 678.2267, found 678.2238.

Synthesis of H_2C_2Ps (*syn*,*syn*-Isomer 3, *syn*,*anti*-Isomer 4, and *anti*,*anti*-Isomer 5). A THF/NMP (1:1, 100 mL) solution of cavitand **6** (550 mg, 520 μmol), porphyrin **8** (160 mg, 236 μmol), and K_2CO_3 (1.0 g) were heated in an autoclave at 120 °C for 4 days. The mixture was evaporated to remove THF. 200 mL of CH_2Cl_2 was added to the mixture, and the organic layer was washed with 1 M HCl and water, and then the solvent was evaporated under reduced pressure. The residue was purified by silica gel column chromatography (benzene). Isomers **3** and **4** of H_2**C$_2$P**s were obtained as the first and second porphyrin fractions in 15 and 34% yield, respectively. The isomer **5** was not obtained.

3: ^{1}H NMR (500 MHz, $CDCl_3$): δ 9.17 (br, 2H, pyrrole-β), 9.10 (br, 2H, pyrrole-β), 8.98 (br, 2H, pyrrole-β), 8.64 (d, $J =$ 6.9 Hz, 4H, Ar–H of porphyrin), 8.33 (br, 2H, pyrrole-β), 7.91–7.83 (m, 10H, Ar–H of porphyrin), 7.23 (d, $J = 8.7$ Hz, 2H, Ar–H of porphyrin), 7.15–7.05 (m, 24H, $CHCH_2H_2$*Ph*), 6.95–6.85 (m, 16H, $CHCH_2H_2$*Ph*), 6.48 (s, 4H, Ar–H of cavitand), 6.30 (s, 4H, Ar–H of cavitand), 5.33 (d, $J = 7.6$ Hz, 2H, H_{co} of –OCH_2O–), 5.13 (d, $J = 7.3$ Hz, 4H, H_{bo} of –OCH_2O–), 4.94 (d, $J = 8.6$ Hz, 4H, –OCH_2Ar– of linker), 4.86 (s, 4H, Ar–H of cavitand), 4.72 (d, $J = 8.6$ Hz, –OCH_2Ar– of linker), 4.35–4.20 (m, 6H, C*H*CH_2CH_2Ph), 4.10 (br, 2H, H_{ao} of –OCH_2O–), 3.99 (t, $J = 7.8$ Hz, 2H, C*H*CH_2CH_2Ph), 2.40–2.10 (m, 18H, $CHCH_2CH_2Ph + H_{ci}$), 2.10–1.90 (m, 16H, $CHCH_2CH_2$Ph), 1.81 (br, 4H, H_{bi} of –OCH_2O–), −0.05 (br, 2H, H_{ai} of –OCH_2O–) −3.41(s, 2H, NH). HR-MS ($C_{176}H_{142}N_4O_{20}$): m/z = calcd 2631.0217, found 2631.0205. Elemental analysis (after reprecipitation from methanol): calcd for $C_{176}H_{142}N_4O_{20}$·2MeOH: C, 79.27; H, 5.61; N, 2.08%. Found: C, 79.17; H, 5.43; N, 2.37%.

4: ^{1}H NMR (500 MHz, $CDCl_3$): δ 9.12 (br, 2H, pyrrole-β), 8.95 (br, 2H, pyrrole-β), 8.87 (s, 2H, Ar–H of porphyrin), 8.55 (br, 2H, pyrrole-β), 8.44 (s, 2H, Ar–H of porphyrin), 8.34 (br, 2H, pyrrole-β), 7.86 (t, $J = 8.4$ Hz, 2H, Ar–H of porphyrin), 7.80 (br, 4H, Ar–H of porphyrin), 7.41 (d, $J = 8.4$ Hz, 2H, Ar–H of porphyrin), 7.14 (d, $J = 8.4$ Hz, 2H, Ar–H of porphyrin), 7.13–7.01 (m, 24H, $CHCH_2H_2$*Ph*), 6.94–6.86 (m, 16H, $CHCH_2H_2$*Ph*), 6.84 (s, 2H, Ar–H of cavitand), 6.70 (br, 2H, Ar–H of porphyrin), 6.54 (s, 2H, Ar–H of cavitand), 6.53 (s, 2H, Ar–H of cavitand), 6.51 (s, 2H, Ar–H of cavitand), 6.48 (s, 2H, Ar–H of cavitand), 6.28 (s, 2H, Ar–H of cavitand), 5.97 (d, $J = 6.9$ Hz, 2H, H_{bo} of –OCH_2O– (anti)), 5.73 (d, 2H, $J = 7.2$ Hz, H_{bo} of –OCH_2O– (syn)), 5.72 (br, 1H, H_{ao} of –OCH_2O– (anti)), 5.25 (br, 1H, H_{co} of –OCH_2O– (syn)), 5.12 (d, $J = 8.0$ Hz, 2H, –OCH_2Ar– of linker (syn)), 4.95 (d, $J = 8.0$ Hz, –OCH_2Ar– of linker (syn)), 4.71 (t, 1H, $J = 8.0$ Hz, C*H*CH_2CH_2Ph (anti)), 4.64 (t, 2H, $J = 8.0$ Hz, C*H*CH_2CH_2Ph (anti)), 4.49 (d, 2H, $J = 7.2$ Hz, H_{bi} of –OCH_2O– (syn)), 4.45–4.40 (m, 3H, H_{bi} of –OCH_2O– (anti) + C*H*CH_2CH_2Ph (anti)), 4.31 (br, 2H, C*H*CH_2CH_2Ph (syn)), 3.94 (br, 1H, C*H*CH_2CH_2Ph (syn)), 3.91 (d, $J = 8.3$ Hz, 2H, –OCH_2Ar– of linker (anti)), 3.57 (d, $J = 8.1$ Hz, 2H, –OCH_2Ar– of linker (anti)), 3.21 (br, 1H, H_{ao} of –OCH_2O– (syn)), 2.95 (t, $J = 8.0$ Hz, 1H, C*H*CH_2CH_2Ph (syn)), 2.84 (br, 1H, H_{ai} of –OCH_2O– (anti)), 2.59–1.50 (m, 33H, $CHCH_2CH_2$Ph + H_{ci} (syn)), 1.03 (br, 1H, H_{co} of –OCH_2O– (anti)), −0.66 (br, 2H, H_{ai} of –OCH_2O– (syn)) −1.70 (br, 1H, H_{ci} of –OCH_2O– (anti)), −2.93 (s, 2H, NH). HR-MS ($C_{176}H_{142}N_4O_{20}$): m/z = calcd 2631.0217, found 2631.0173. Elemental analysis (after reprecipitation from methanol): calcd for $C_{176}H_{142}N_4O_{20}$·MeOH: C, 79.77; H, 5.52; N, 2.10%. Found: C, 79.71; H, 5.62; N, 2.08%.

^{1}H NMR Titrations for Determination of Guest Association Constants. The $CDCl_3$ solution of H_2**C$_2$P**s (2 mM for **3**, 5 mM for **4**, 0.6 mL) was placed into a J Young® gas-tight NMR tube with a valve. Guest hydrocarbon gases were introduced into the solution directly by syringe. The guest association constants K_{11} and K_{12} in H_2**C$_2$P**s were determined by ^{1}H NMR spectra at various guest concentrations (1–120 mM) at 25 °C. Ratios between the free ([G]) and total amount of encapsulated ($[G]_{in}$) guests were determined by the integration of their proton signals based on those of the host signals as a reference. Free host concentration [H] was estimated from the amount of entrapped guest. The K_{11} values for **4** were calculated by the eq 1. The results are shown in Table 1 and Figure S1. The 1:1 and 1:2 association constants for **3** were obtained by nonlinear least square curb fittings on KaleidaGraph® software with eq 7 which is delivered from eqs 1–4 as eqs 5 and 6. The curve fittings are shown in Figure S6.

$$K_{11} = \frac{[H\cdot G]}{[H][G]} \quad (1)$$

$$K_{12} = \frac{[H\cdot G_2]}{[H\cdot G][G]} \quad (2)$$

$$[H]_o = [H] + [H\cdot G] + [H\cdot G_2] \quad (3)$$

$$[G]_o = [G] + [H\cdot G] + 2[H\cdot G_2] \quad (4)$$

$$[H] = \frac{[H]_o}{1 + K_{11}[G] + K_{11}K_{12}[G]^2} \quad (5)$$

$$[G]_{in} = [H\cdot G] + 2[H\cdot G_2]$$
$$= \{K_{11}[G] + 2K_{11}K_{12}[G]^2\}[H] \quad (6)$$

$$[G]_{in} = \frac{K_{11}[G] + 2K_{11}K_{12}[G]^2}{1 + K_{11}[G] + K_{11}K_{12}[G]^2}[H]_o \quad (7)$$

This work was supported by the Grants-in-Aid for Scientific Research on Priority Areas (No. 15036254) from MEXT and Scientific Research (A)/(S) (Nos. 14204073 and 17105003) and for Exploratory Research (No. 16655039) from JSPS as well as by a grant from The Asahi Glass Foundation. J. N. acknowledges JSPS Research Fellowship.

Supporting Information

The plots and curve fittings for determination of association constants (Figures S1 and S6). ^{1}H NMR spectral changes upon encapsulation of acetylene, ethylene, cyclopropane, and propane into **3** (Figures S2–S5). Assignments of ^{1}H–^{1}H COSY spectra of host **3** and **4** (Figures S7 and S8). This material is available free of charge on the web at: http://www.csj.jp/journals/bcsj/.

References

1 J.-M. Lehn, *Supramolecular Chemistry: Concepts and Prespectives*, VCH, Weinheim, **1995**.
2 D. M. Rudkevich, *Angew. Chem., Int. Ed.* **2004**, *43*, 558.
3 M. Fujita, K. Umemoto, M. Yoshizawa, N. Fujita, T. Kusukawa, K. Biradha, *Chem. Commun.* **2001**, 509.
4 D. Fiedler, D. H. Leung, R. G. Bergman, K. N. Raymond, *Acc. Chem. Res.* **2005**, *38*, 349.
5 L. Avram, Y. Cohen, J. Rebek, Jr., *Chem. Commun.* **2011**, *47*, 5368.
6 P. Jin, S. J. Dalgarno, J. L. Atwood, *Coord. Chem. Rev.* **2010**, *254*, 1760.
7 S. J. Dalgarno, N. P. Power, J. L. Atwood, *Coord. Chem. Rev.* **2008**, *252*, 825.
8 D. M. Vriezema, M. C. Aragones, J. A. A. W. Elemans, J. J. L. M. Cornelissen, A. E. Rowan, R. J. M. Nolte, *Chem. Rev.* **2005**, *105*, 1445.
9 D. M. Rudkevich, *Bull. Chem. Soc. Jpn.* **2002**, *75*, 393.
10 J. Rebek, Jr., *Angew. Chem., Int. Ed.* **2005**, *44*, 2068.
11 F. Hof, S. L. Craig, C. Nuckolls, J. Rebek, Jr., *Angew. Chem., Int. Ed.* **2002**, *41*, 1488.
12 T. Haino, M. Kobayashi, Y. Fukazawa, *Chem.—Eur. J.* **2006**, *12*, 3310.
13 T. Haino, M. Hirakata, K. Niimi, M. Kouchi, H. Iwamoto, Y. Fukazawa, *Chem. Lett.* **2008**, *37*, 394.
14 P. Ballester, G. Gil-Ramírez, *Proc. Natl. Acad. Sci. U.S.A.* **2009**, *106*, 10455.
15 H. Kitagawa, Y. Kobori, M. Yamanaka, K. Yoza, K. Kobayashi, *Proc. Natl. Acad. Sci. U.S.A.* **2009**, *106*, 10444.
16 D. Ajami, J.-L. Hou, T. J. Dale, E. Barrett, J. Rebek, Jr., *Proc. Natl. Acad. Sci. U.S.A.* **2009**, *106*, 10430.
17 J. Sun, B. O. Patrick, J. C. Sherman, *Tetrahedron* **2009**, *65*, 7296.
18 C. L. D. Gibb, B. C. Gibb, *Tetrahedron* **2009**, *65*, 7240.
19 H. Kitagawa, M. Kawahata, R. Kitagawa, Y. Yamada, M. Yamanaka, K. Yamaguchi, K. Kobayashi, *Tetrahedron* **2009**, *65*, 7234.
20 M. Yamanaka, M. Kawaharada, Y. Nito, H. Takaya, K.

Kobayashi, *J. Am. Chem. Soc.* **2011**, *133*, 16650.
21 N. Nishimura, K. Yoza, K. Kobayashi, *J. Am. Chem. Soc.* **2010**, *132*, 777.
22 K. Kobayashi, R. Kitagawa, Y. Yamada, M. Yamanaka, T. Suematsu, Y. Sei, K. Yamaguchi, *J. Org. Chem.* **2007**, *72*, 3242.
23 N. Branda, R. Wyler, J. Rebek, Jr., *Science* **1994**, *263*, 1267.
24 R. M. Grotzfeld, N. Branda, J. Rebek, Jr., *Science* **1996**, *271*, 487.
25 R. S. Meissner, J. Rebek, Jr., J. de Mendoza, *Science* **1995**, *270*, 1485.
26 S. D. Starnes, D. M. Rudkevich, J. Rebek, Jr., *J. Am. Chem. Soc.* **2001**, *123*, 4659.
27 S. Mecozzi, J. Rebek, Jr., *Chem.—Eur. J.* **1998**, *4*, 1016.
28 B. W. Purse, J. Rebek, Jr., *Proc. Natl. Acad. Sci. U.S.A.* **2005**, *102*, 10777.
29 S. Arai, H. Ohkawa, S. Ishihara, T. Shibue, S. Takeoka, H. Nishide, *Bull. Chem. Soc. Jpn.* **2005**, *78*, 2007.
30 T. Haino, T. Fujii, A. Watanabe, U. Takayanagi, *Proc. Natl. Acad. Sci. U.S.A.* **2009**, *106*, 10477.
31 T. Haino, K. Fukuta, H. Iwamoto, S. Iwata, *Chem.—Eur. J.* **2009**, *15*, 13286.
32 A. K. Sundaresan, C. L. D. Gibb, B. C. Gibb, V. Ramamurthy, *Tetrahedron* **2009**, *65*, 7277.
33 T. Haino, E. Hirai, Y. Fujiwara, K. Kashihara, *Angew. Chem., Int. Ed.* **2010**, *49*, 7899.
34 H. Iwamoto, S. Nishi, T. Haino, *Chem. Commun.* **2011**, *47*, 12670.
35 N. Nishimura, K. Kobayashi, *J. Org. Chem.* **2010**, *75*, 6079.
36 D. M. Rudkevich, W. Verboom, D. N. Reinhoudt, *J. Org. Chem.* **1995**, *60*, 6585.
37 O. Middel, W. Verboom, D. N. Reinhoudt, *J. Org. Chem.* **2001**, *66*, 3998.
38 H. Iwamoto, Y. Yukimasa, Y. Fukazawa, *Tetrahedron Lett.* **2002**, *43*, 8191.
39 X. Liu, J. Sun, R. Warmuth, *Tetrahedron* **2009**, *65*, 7303.
40 A. Shivanyuk, J. Rebek, Jr., *J. Am. Chem. Soc.* **2003**, *125*, 3432.
41 O. Molokanova, G. Podoprygorina, M. Bolte, V. Böhmer, *Tetrahedron* **2009**, *65*, 7220.
42 L. R. MacGillivray, J. L. Atwood, *Nature* **1997**, *389*, 469.
43 J. L. Atwood, L. J. Barbour, A. Jerga, *Proc. Natl. Acad. Sci. U.S.A.* **2002**, *99*, 4837.
44 M. Yoshizawa, M. Fujita, *Pure Appl. Chem.* **2005**, *77*, 1107.
45 M. Yoshizawa, M. Tamura, M. Fujita, *Science* **2006**, *312*, 251.
46 A. B. C. Deutman, C. Monnereau, M. Moalin, R. G. E. Coumans, N. Veling, M. Coenen, J. M. M. Smits, R. de Gelder, J. A. A. W. Elemans, G. Ercolani, R. J. M. Nolte, A. E. Rowan, *Proc. Natl. Acad. Sci. U.S.A.* **2009**, *106*, 10471.
47 T. Amaya, J. Rebek, Jr., *Chem. Commun.* **2004**, 1802.
48 A. Shivanyuk, A. Scarso, J. Rebek, Jr., *Chem. Commun.* **2003**, 1230.
49 L. C. Palmer, Y.-L. Zhao, K. N. Houk, J. Rebek, Jr., *Chem. Commun.* **2005**, 3667.
50 D. Ajami, M. P. Schramm, J. Rebek, Jr., *Tetrahedron* **2009**, *65*, 7208.
51 T. Heinz, D. M. Rudkevich, J. Rebek, Jr., *Nature* **1998**, *394*, 764.
52 A. Shivanyuk, J. Rebek, Jr., *J. Am. Chem. Soc.* **2002**, *124*, 12074.
53 C. Ihm, E. Jo, J. Kim, K. Paek, *Angew. Chem., Int. Ed.* **2006**, *45*, 2056.
54 J. M. Rivera, T. Martín, J. Rebek, Jr., *Science* **1998**, *279*, 1021.
55 M. Yamanaka, K. Ishii, Y. Yamada, K. Kobayashi, *J. Org. Chem.* **2006**, *71*, 8800.
56 N. P. Power, S. J. Dalgarno, J. L. Atwood, *New J. Chem.* **2007**, *31*, 17.
57 D. Ajami, J. Rebek, Jr., *Angew. Chem., Int. Ed.* **2008**, *47*, 6059.
58 J. Nakazawa, J. Hagiwara, M. Mizuki, Y. Shimazaki, F. Tani, Y. Naruta, *Angew. Chem., Int. Ed.* **2005**, *44*, 3744.
59 J. Nakazawa, M. Mizuki, J. Hagiwara, Y. Shimazaki, F. Tani, Y. Naruta, *Bull. Chem. Soc. Jpn.* **2006**, *79*, 1431.
60 J. Nakazawa, M. Mizuki, Y. Shimazaki, F. Tani, Y. Naruta, *Org. Lett.* **2006**, *8*, 4275.
61 J. Nakazawa, Y. Sakae, M. Aida, Y. Naruta, *J. Org. Chem.* **2007**, *72*, 9448.
62 A. Bellelli, M. Brunori, A. E. Miele, G. Panetta, B. Vallone, *Curr. Protein Pept. Sci.* **2006**, *7*, 17.
63 D. H. Williams, E. Stephens, D. P. O'Brien, M. Zhou, *Angew. Chem., Int. Ed.* **2004**, *43*, 6596.
64 F. Tani, M. Matsu-ura, S. Nakayama, M. Ichimura, N. Nakamura, Y. Naruta, *J. Am. Chem. Soc.* **2001**, *123*, 1133.
65 M. Nishino, M. Hirota, Y. Umezawa, *The CH/π Interaction*, Wiley-VCH, New York, **1998**.
66 A. Brown, *Int. J. Mol. Sci.* **2009**, *10*, 3457.